Proceedings of the International Conference
Nanomaterials: Applications and Properties
Vol. 4 No 2, 02NABM05(8pp) (2015)

Heme-protein Modified Electrodes for Highly Selective and Sensitive Detection of H_2O_2 from Apple Juice

Naeem Akhtar[1,2], Sherif A. El-Safty[1,2,*], Mamdouh E. Abdelsalam[3]

[1] *National Institute for Materials Science (NIMS), 1-2-1 Sengen, Tsukuba-shi, Ibaraki-ken 305-0047, Japan*
[2] *Graduate School of Advanced Science and Engineering, Waseda University, 3-4-1 Okubo, Shinjuku-Ku, Tokyo,169-8555, Japan*
[3] *Malmesbury, SN16 0RP, United Kingdom*

(Received 01 June; published online 29 August 2015)

The development of an accurate, sensitive, and selective hydrogen peroxide (H_2O_2) diagnostic device with a low detection limit is important in the fields of biology and medicine. Numerous approaches have been reported for electrochemical detection of H_2O_2. These approaches exhibit good stability and selectivity with a low detection limit, but involve a complicated fabrication process. We designed and fabricated three enzyme-free H_2O_2 biosensors by coating a three-dimensional open-pore nickel foam (3D-Ni foam) electrode with heme proteins, namely, (hemoglobin (Hb), myoglobin (Mb), and cytochrome c (Cyt.c)). The heme protein-modified Ni foam can be directly used as electrodes, thereby simplifying the electrode fabrication process and offering advantages, such as enhanced electrode–electrolyte contact area and minimum diffusion resistance. Heme proteins can function as a redox mediator for shuttling electrons on the electrode–electrolyte interface and for engaging sufficient electro-active species exposed on the surface of the Ni foam for the Faradaic redox reaction. The immobilization of the heme proteins onto the 3D Ni foam was analyzed using scanning electron microscopy, UV-visible spectroscopy, contact angle, and Raman spectroscopy. The heme proteins maintained their biological functions and effective electronic connection and affected the interfacial properties of the Ni foam after immobilization. The electrochemical effects of the Ni foam electrodes modified with similar concentrations of different heme proteins (Hb, Mb, and Cyt.c) in the selective oxidation of H_2O_2 were investigated and compared. Hence, these electrodes can be applied in the analysis of real samples, such as apple juice.

Keywords: Hydrogen peroxide; Electrochemical sensor; Hemoglobin; Cytochrome c; Myoglobin; Interfacial properties.

PACS numbers: 87.85.fk, 82.47.Rs

1. INTRODUCTION

The development of support materials for the efficient adsorption of proteins on a solid surface is important for fabricating biosensors and bioreactors [1]. Biosensors with biological recognition components, such as organisms or biological materials, are essential tools for detecting and monitoring the parameters involved in physiological or biochemical processes. Biosensors for biomedical applications can be coupled to a physico-chemical transducer that converts the recognition into a detectable output signal and can provide a comprehensive review of the established, cutting-edge, and future trends in biomedical sensors and their applications [2]. The proteins/enzymes immobilized on a solid support can rapidly terminate the reaction through removal of the immobilized proteins from the reaction solution, thereby significantly lowering the cost because the product is not contaminated with the protein [3]. In addition, the matrix should allow easy access of substrates in solution to the immobilized proteins to promote the catalytic reaction. Porous materials with two- and three-dimensional (2D and 3D, respectively) architectures have received an enormous amount of attention because of their high surface area and tunable and uniform pore size; these materials are considered versatile hosts for numerous guest molecules, such as proteins, drugs, and small biological molecules [4–7]. A previous study showed that electrodes modified with conductive porous layers can change the mass transport regime from "linear diffusion" to an approximately "thin layer" characteristic. This modification can optimize the potential at which target species undergo redox processes; hence, the resulting electrodes facilitate the differentiation between the species that can be oxidized or reduced at similar potentials under planar diffusion conditions [8, 9].

A three-dimensional porous nickel (3D Ni) foam substrate has received enormous interest over the recent years because of its extraordinary electrical properties, excellent mechanical strength, inertness, relatively low toxicity, ease of production scale-up, low cost, and high corrosion stability in aqueous alkaline media [10]. In addition, the open-pore architecture of the 3D Ni foam contains an interpenetrating network of electrons and ion pathways that allows efficient kinetics of ion and electron transport in the electrodes and at the electrode–electrolyte interface [11]. Therefore, the 3D Ni foam is an ideal electrode architecture for highly sensitive detection of biomolecules, such as glucose and H_2O_2. The electrode surface should be engineered with a large amount of electroactive sites and high transport rates for electrolyte ions and electrons, which participate in the Faradic redox reactions, to maximize the electrochemical performance [12]. A large specific surface area of the electroactive materials is required to

* sherif.elsafty@nims.go.jp

accommodate a large amount of superficial electroactive species that will participate in the Faradaic redox reactions. Moreover, the high transport rates entail fast diffusion of the electrolyte ions and fast conduction of electrons to the electroactive sites. This structure can be achieved by developing porosity in an electroactive material with a large surface area, high electrical conductivity, and fast ion transport [13]. The safe immobilization of heme proteins on the surface of the Ni-foam working electrode can enhance the surface active sites of the porous Ni foam [14]. Heme proteins are distinctively characterized by their stability over a wide pH range and their significant function as a biological electron-transport chain [15] with peroxidase-like activity [16] in a biosensor design.

Initiation and progression of many diseases are indirectly linked to several oxidative stress-related states [17]. Hydrogen peroxide (H_2O_2) is a reactive oxygen metabolic byproduct of several processes involving oxidases, such as glucose oxidase, cholesterol oxidase, glutamate oxidase, urate oxidase, lactate oxidase, alcohol oxidase, d-amino acid oxidase, lysine oxidase, and oxalate oxidase [18]. Therefore, many analytical techniques (visible absorption spectrometry, spectrofluorometry, chemiluminescence, and electrochemical analysis) have been used to detect H_2O_2 [19–22]. Electrochemical technique is a convenient method for H_2O_2 detection because of its fast response time and satisfactory sensitivity and selectivity [23].

The development of non-enzymatic H_2O_2 electrochemical sensors was the focus of previous research because these sensors do not have the limitations (high cost and low thermal stability) of enzyme-based sensors [24]. Several modified electrodes based on Prussian blue, platinum, helical carbon nanotubes, and different transition metal oxides have been efficiently used to develop non-enzymatic H_2O_2 sensors [25–28]. However, most of these electrodes suffer from low stability, poor reusability, and complicated preparation process [29]. Therefore, a simple design for a highly sensitive and selective H_2O_2 electrochemical sensor must be developed to detect ultra-low concentrations of H_2O_2 in real samples with high flexibility.

We previously fabricated a highly selective non-enzymatic amperometric sensor based on Cyt.c- and Hb-modified porous Ni-foam electrodes for H_2O_2 detection [30, 31]. In the present work, the differences in the signaling and stability of electrochemical H_2O_2 sensors were compared. The sensors were fabricated using three different heme proteins (Hb, Mb, and Cyt.c) to modify the 3D open-pore Ni foam-based electrodes. We further investigated the effects of the different biofunctionalities of these heme proteins on the interfacial properties of the immobilized substrate, thereby enhancing the exposed electroactive species for the Faradic redox reaction. Our findings revealed that the Ni foam electrodes modified with non-enzymatic heme proteins exhibited a wide working range, excellent selectivity, high sensitivity, and low detection limits. These interesting features of the Ni-foam electrodes modified with heme proteins suggested new prospects for the future development of a low cost and highly sensitive electrochemical sensor for H_2O_2.

2. EXPERIMENTAL SECTION

2.1 Materials and reagents

All chemicals were of analytical grade and were used without further purification. Hb, Mb, Cyt.c, uric acid (UA), H_2O_2 aqueous solution (30% v/v), hydrochloric acid (HCl), potassium ferricyanide ($K_3Fe(CN)_6$), and phosphate buffer saline were purchased from Sigma–Aldrich Company, Ltd., USA. Sodium hydroxide (NaOH) and L(+)-ascorbic acid (AA) were obtained from Wako Company, Ltd., Osaka, Japan. The commercial 3D porous Ni foam was purchased from Nilaco Corporation Tokyo, Japan. A pack of apple juice was obtained from a local supermarket (Tsukuba, Japan). The apple juice (pH 3.0) contained sucrose, citrate, malic acid, essence, caramel, apple juice concentrate, and water.

2.2 Fabrication of the Ni-foam electrodes modified with heme proteins

Heme protein-modified electrodes were fabricated by immobilizing the heme proteins onto the Ni-foam electrode. First, the Ni foam was carefully cleaned with a concentrated HCl solution (2 M) in an ultrasound bath for 5 min to remove the NiO layer on the surface. Deionized water and absolute ethanol were used for 5 min each to ensure that the Ni foam surface was completely clean. In the second step, we immobilized a specific amount (100 μM) of the heme proteins onto the surface of the Ni foam electrode. In the third step, we dried the resulting Ni-foam electrode modified with heme proteins at 60 °C overnight prior to electrochemical analysis.

2.3 Instrumentation

A Zennium/ZAHNER-Elektrik instrument controlled by Thales Z 2.0 software was used for electrochemical measurements at room temperature. A conventional three-electrode system consisting of a heme protein-modified Ni foam/Ni foam (1 mm × 1 cm × 2 cm) working electrode, a platinum wire counter electrode, and Ag/AgCl (3 M NaCl) reference electrode was used for analysis.

2.4 Material characterization

The morphology and chemical composition of the Ni foam and heme protein-modified Ni foam were investigated with TM-3000 equipped with an energy-dispersive X-ray micro analyzer (EDX) at an accelerating applied potential of 15 keV. The Ni foam substrates were fixed on the SEM stage by using carbon tapes, after which the substrates were inserted into the chamber. The Pt films were deposited on the substrates at room temperature through ion sputtering (Hitachi E-1030). The distance between the target and the substrate was 5.0 cm. The sputtering deposition system consisted of a stainless steel chamber evacuated to 8×10^{-5} Pa with a turbo-molecular pump and backed up by a rotary pump. The Pt target (8 nm diameter, purity 99.95%) was sputter cleaned in pure Ar before sputtering deposition. The Ar working pressure (2.8×10^{-1} Pa), power supply (100 W), and deposition rate were maintained constant throughout the investigation.

The absorbance spectra of the bare Ni foam and the

Ni-foam electrodes modified with heme proteins were determined with a UV-Vis-NIR spectrophotometer (Shimadzu 3700). The immobilization of heme proteins onto the Ni foam was confirmed using Raman spectroscopy with Raman Horiba (XploRA™ PLUS, France). Raman spectra were recorded using an Ar-ion laser emitting light at 533 nm wavelength. A camera detection system containing a charge-coupled device and an analyzing software package (LabSpec_3.01C) was used for data acquisition. Ten scans of 5 s each from 400 cm^{-1} to 1,700 cm^{-1} were recorded, and the average was obtained.

Static water contact angles (WCAs) on the surfaces of the bare Ni foam and Ni-foam electrodes modified with heme proteins were measured at room temperature with a contact angle analysis equipment (VCA Optima, AST Products, Inc., USA) through the sessile drop method with 100 μL of water droplet. WCA values were recorded after 3 s from droplet deposition.

2.5 Real sample analyses

Real sample analysis was performed using commercially available apple juice. Standard titration method (KMnO4) was used to confirm whether the apple juice contained endogenous H_2O_2 prior to the determination. A standard concentration of H_2O_2 was injected into the test solution to determine the concentration of H_2O_2 in the apple juice sample. The mixed sample was analyzed using the Ni-foam electrode modified with heme proteins. Response current was recorded when the steady state was reached. The difference between the baseline and the steady state current was used to calculate the H_2O_2 concentration.

3. RESULTS AND DISCUSSION

3.1 Structural features of the Ni-foam electrodes modified with heme proteins

The successful immobilization of heme proteins onto the 3D Ni foam may not only reduce the diffusion resistance of the electrolyte, but also enhance the ion transmission performance because of the increased number of surface active sites, as shown in the SEM profile, UV-Vis absorbance spectrum, Raman spectroscopy, and WCA analyses. The structures of the Ni foam and Ni-foam substrates modified with heme proteins were analyzed using SEM. Fig. 1 shows the typical SEM micrographs of the Ni foam before and after modification with heme proteins. The Ni foam exhibited a 3D cross-linked structure with a pore size of few 100 μm (Fig. 1A). The high-magnification SEM image revealed the compact structure of the interconnected grain-like vertebrae with narrow grain boundaries (Fig. 1B). The 3D porous structure of the Ni foam provided high accessibility and rapid transport of electrons and ions. The modification of the porous 3D Ni foam with hemeproteins (Fig. 1C) resulted in the formation of a film on the surface of the foam because of the high binding interactions between the Ni-based material and the heme proteins [10]. The high-magnification SEM micrographs of the hemeprotein modified Ni foam (Figs. 1D) revealed the covered and uncovered surface of the Ni foam electrodes. The EDX mapping distribution of the heme-protein (Mb) film on the Ni foam are shown in Fig. 2 (a–d). EDX map showed a 3D porous network consisting of Ni, C, Fe, and O atoms (O not shown). The Ni atoms were uniformly distributed on the entire surface area of the Ni foam. C, O, and Fe atoms were the components of the heme protein (Mb). This elemental ratio of the heme protein-modified Ni foam indicated that the Ni foam was in pure metallic form.

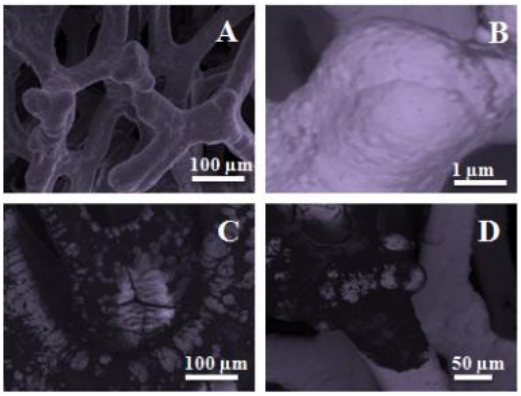

Fig. 1 – Fe-SEM images of the bare Ni foam, (A & B) and Heme-protein modified Ni foam electrode (C & D).

The immobilization of the heme protein moieties onto the porous surfaces of the Ni foam was determined using spectroscopic UV-Vis and Raman techniques. The UV-Vis spectra (Fig. 3A) showed the functionalized heme protein onto the Ni foam during the fabrication of the 3D porous heme protein-modified Ni-foam electrode. The presence of Soret absorption bands at around 409 cm^{-1} for Mb and Cyt.c and 405 cm^{-1} for Hb was attributed to the impregnation of the porphyrin chromophore of the heme proteins onto the Ni foam, as demonstrated by the free heme protein absorption bands in the solution [32].

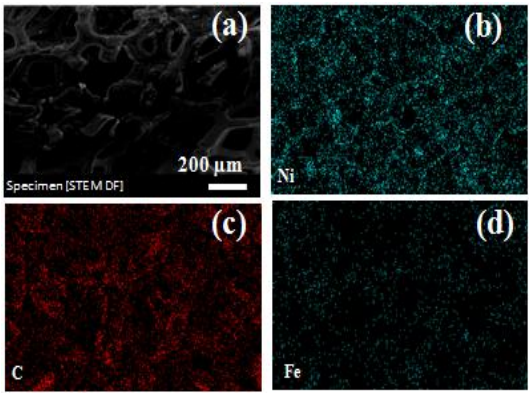

Fig. 2 – SEM–EDX mapping of the Mb film in the Ni Foam electrode: (a) SEM image and the distribution of nickel (b), carbon (c) and iron (d).

The Raman spectrum of the Hb/Ni foam (Fig. 3B-c) was characterized by the presence of an intense band near 1,382 cm^{-1}, which was a marker for the symmetric stretching vibrations of Fe^{3+} of Hb and for the liganded ferro forms (a six-coordinated heme). This finding is in good agreement with the results of previous reports [33, 34]. The other prominent Raman bands at around 1,000 cm^{-1} could be correlated with the phenyl mode of the aromatic amino acid residues. The Raman spec-

trum of the Hb/Ni foam was characterized by three prominent Hb bands at 1,375, 1,586, and 1,650 cm^{-1}, which were the "markers of the hemic group packed in the polypeptidic chain" and were assigned to the "in plane vibrations of the porphyrine ring" [35, 36]. In addition, the dominant Raman bands located at 1,572, 1,586, and 1,615 cm^{-1} were assigned to the C=C and C=N symmetric stretching vibration modes. The bands located at 674 and 784 cm^{-1} are related to the porphyrine bending vibrations out of the plane.

The Raman spectrum of the Mb/Ni foam (Fig. 3B-b) was consistent with those reported in literature [37]. The bands at 1,370, 1,480, and 1,551 cm^{-1} were characteristics of a ferric six-coordinated high-spin heme species. The bands at 1,542, 1,585, and 1,622 cm^{-1} represented the vinyl stretching. In addition, the bending modes of the vinyl and propionate groups were observed at 407 and 458 cm^{-1}, respectively.

The Raman spectrum of the Cyt.c/Ni foam (Fig. 3B-a) showed characteristic peaks at 271 and 347 cm^{-1}, which could be attributed to the metal-N (pyrrole) stretching and pyrrole substituent bending coordinates, respectively. In addition, the Raman peak at 692 cm^{-1} represented the stretching vibration corresponding to the pyrrole ring. However, the two peaks at 750 and 1,634 cm^{-1} could be assigned to the pyrrole breathing mode stretching vibration in the C–H and amide I band of the protein, respectively [38, 39] . Moreover, the two peaks at 1,120 and 1,231 cm^{-1} were assigned to the C–H bending mode.

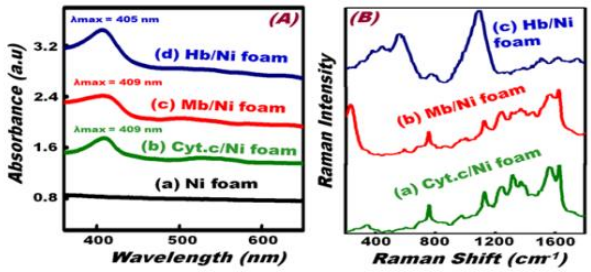

Fig. 3 – (A) UV-Vis absorption spectra of the (a) bare Ni foam, (b) Cyt.c/Ni foam, (c) Mb/Ni foam, and (d) Hb/Ni foam. (B) Raman spectra of the (a) Cyt.c/Ni foam, (b) Mb/Ni foam, and (c) Hb/Ni foam.

3.2 Electrochemical behavior of the Ni-foam electrodes modified with heme proteins

We first examined the surface of the bare Ni foam and Ni foam-electrodes modified with heme proteins through cyclic voltammetry in a buffer solution (pH = 7.0) containing 5 mM $(Fe(CN)_6)^{3-/4-}$ within the potential range of 0.0 V to 1.0 V (vs. Ag|AgCl) and at a scan rate of 100 mV/s (Fig. 4A). The magnitude of the current is higher for the heme protein-modified Ni foam electrode than that for the bare Ni foam. This finding is due to the enhanced ion transmission performance at the electrode-electrolyte interface, thereby engaging a sufficient number of electro-active species exposed at the electrode-electrolyte interface for the Faradaic redox reaction. However, the Mb- and Hb-modified Ni-foam electrodes exhibited lower current response than the Cyt.c modified Ni-foam electrode. The reduced electrochemical signal could be attributed to the decreased mass transport of the ferricyanide ions caused by the molecular recognition process [40].

We subsequently measured the electron-transfer rate through the cyclic voltammetry (CV) responses (Fig. 4B) of the bare Ni foam, Hb/Ni foam, Mb/Ni foam, and Cyt.c/Ni foam electrodes in 0.1 M NaOH solution at a scan rate of 100 mV/s. The CV curves of all electrodes showed asymmetrical redox peaks. The peak-to-peak separation values (ΔE_p) of the bare Ni foam, Hb/Ni foam, Mb/Ni foam, and Cyt.c/Ni foam were 0.21, 0.17, 0.17, and 0.16 V, respectively. The small ΔE_p values of the Ni foam modified with heme proteins indicated a faster electron-transfer rate and increased reversibility compared with the sensing system of the bare Ni foam [Scheme 1].

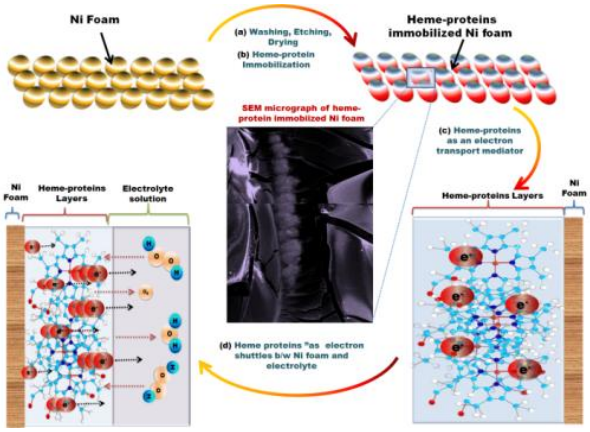

Scheme 1 – A schematic illustration of heme proteins as electron shuttles between the Ni foam and electrolytes.

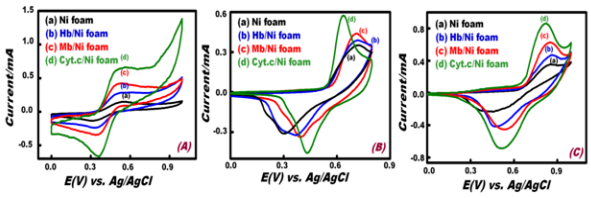

Fig. 4 – Typical CV patterns of the (a) bare Ni foam, (b) Hb/Ni foam, (c) Mb/Ni foam, and (d) Cyt.c/Ni foam in (A) a buffer solution (pH = 7.0) containing 5 mM $(Fe(CN)_6)^{3-/4}$, (B) 0.1 M NaOH solution, and (C) 0.1 M NaOH solution containing 1 mM H_2O_2 at a scan rate of 100 mV/s.

To explore the effect of the formation type of redox species on the electrode surface, we examined the CV response of the bare Ni foam and heme protein-modified Ni foam electrodes in alkaline solution containing 1 mM H_2O_2 at a scan rate of 100 mV/s (Fig. 4C). The anodic oxidation of the Ni foam was related to the $Ni/Ni(OH)_2$ and $Ni(OH)_2/NiOOH$ redox reactions in our working electrode, as presented in a previous study [41]. Our findings reveal that the weak anodic peak at 0.45 V and the strong anodic peak at 0.81 V (vs. Ag|AgCl) corresponded to the oxidation of Ni to $Ni(OH)_2$ and to that of $Ni(OH)_2$ to NiOOH species, respectively. In the cathodic sweep-based process, the strong peak at 0.51 V was due to the reduction of NiOOH to $Ni(OH)_2$ [42]. $Ni(OH)_2$ could exist in two crystallographic forms, namely, the hydrous α-$Ni(OH)_2$ and the anhydrous ß-$Ni(OH)_2$ [43]. Therefore, the strong anodic (0.81 V) and cathodic peaks (0.51 V) could be related to the formation of the $Ni(OH)_2$/NiOOH redox couple. In turn, because of the instability of α-$Ni(OH)_2$ phase and the transformation tendency to change to ß-phase in alkali solution (i.e., 0.1 M NaOH), the weak anodic peak cen-

tered at 0.45 V could be due to the conversion of hydrous α-Ni(OH)$_2$ to anhydrous ß-Ni(OH)$_2$ [44]. The Ni-foam electrodes modified with heme proteins exhibited a higher current response than that of the bare Ni-foam electrode, thereby indicating that heme proteins enhanced surface activation and electron transfer. The surface activation of heme proteins was attributed to the stable heme cofactor over a wide pH range [15]. The heme group comprised a ring of conjugated double bonds that surround the iron atom. The 3D structure of heme proteins showed that the hydrophobic amino acid cluster was embedded inside the molecule, whereas the hydrophilic residues were positioned on the molecular surfaces. This configuration increased the hydrophilicity of the electrode surface and increased the number of active sites compared with the Ni-foam sensing system [45].

3.3 Functionality of the Ni-foam electrodes modified with heme proteins

Interfacial properties of the Ni-foam electrodes modified with heme proteins.

The interfacial properties (surface energy and wettability) of the different Ni-foam electrodes modified with heme proteins were characterized through contact-angle measurements and subsequently compared with those of the bare Ni foam. The water contact angle (Fig. 5) of the bare Ni foam, Hb/Ni foam, Mb/Ni foam, and Cyt.c/Ni foam were 120.45°, 109.45°, 100.05°, and 87.8°, respectively. In addition, the surface energies of the bare Ni foam and the Ni foams modified with heme proteins were calculated using Girifalco–Good–Fowkes–Young equation [Eq. (1)] [46]. Table 1 shows that the surface energy and surface tension of the bare Ni foam increased after modification with heme proteins.

$$\gamma_{sv} = \gamma_{lv} (1 + \cos\theta)^2/4 \qquad (1)$$

where γ_{sv} and γ_{lv} are the interfacial surface energies of the solid–vapor and liquid–vapor interfaces, respectively. A surface energy of 72.5 mJ m^{-2} for deionized water was used for γ_{lv}, whereas the measured value of the contact angle (θ) was used for γ_{sv} [47]. These results

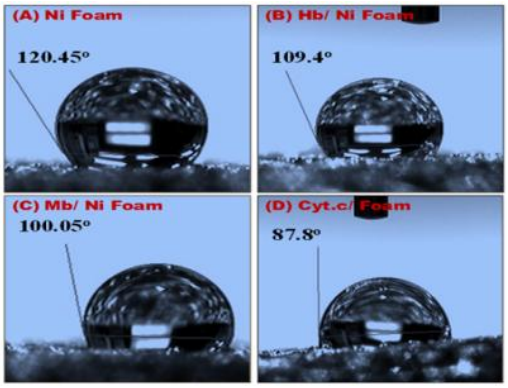

Fig. 5 – Optical images of a water droplet on the surface of the (A) bare Ni foam, (B) Hb/Ni foam, (C) Mb/Ni foam, and (D) Cyt.c/Ni foam.

clearly demonstrated that heme proteins could enhance the hydrophilicity of the Ni foam surface. The increased hydrophilicity of the Ni-foam electrodes modified with heme proteins could enhance the mass-transfer rate at the interface.

Table 1 – Contact angle, surface energy and surface tension of the bare Ni foam and heme-protein (Hb, Mb, Cyt.c) modified Ni foam.

Sensor	Linearity (μM)	LOD (μM)	Sensitivity ($\mu A\ mM^{-1}\ cm^{-2}$)	Time response (s)
Ni foam	50–450	2.25	0.01	5
Hb/Ni foam	50–850	0.80	0.13	3
Mb/Ni foam	50–850	0.73	0.16	3
Cyt.c/Ni foam	50–950	0.20	0.39	3

Effective diffusivity in the porous Ni-foam electrodes modified with heme proteins

The diffusion coefficients of H_2O_2 in the Ni-foam sensors modified with heme proteins and the bare Ni foam were calculated via chronoamperometry (Fig. 6). Chronoamperograms were obtained at 1 mM H_2O_2 (Fig. 6A). Cottrell equation [Eq. (2)] was used to calculate the diffusion coefficient [48]. Fig. 6B reveals that I_t and $t^{1/2}$ exhibit a linear behavior for 1 mM H_2O_2.

$$I_t = nFAD^{1/2}c\pi^{-1/2}t^{-1/2}, \qquad (2)$$

where $I_t(A)$ is the current in the presence of 1 mM H_2O_2, F is the Faraday constant (96,485 C/mol), A is the geometric surface area of the electrode (1 cm^2), D is the diffusion coefficient (cm^2/s), c is the analyte concentration (0.001 mol/cm^3), and t is the elapsed time (s). The Cyt.c/Ni foam electrode presented a higher diffusion coefficient (4.93×10^{-6} cm^2/s) than the Mb/Ni foam (2.12×10^{-6} cm^2/s), Hb/Ni foam (1.33×10^{-6} cm^2/s), and bare Ni foam (0.72×10^{-6} cm^2/s) electrodes. Among all heme proteins, Cyt.c not only efficiently reduced the diffusion resistance of the electrolyte, but also effectively functioned as a mediator, thereby confirming the findings of Bunea et al. [49].

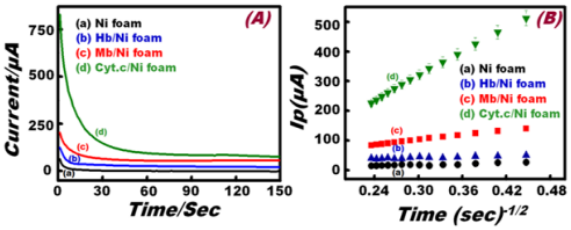

Fig. 6 – (A) Chronoamperograms obtained from the (a) bare Ni foam, (b) Hb/Ni foam, (c) Mb/Ni foam, and (d) Cyt.c/Ni foam in the presence of 1 mM H_2O_2 in 0.1 M NaOH solution. (B) Relationship between current and time$^{-1/2}$ derived from the chronoamperogram data.

3.3.1 Sensitivity of the Ni-foam sensor modified with heme proteins

To compare the sensing applicability of the heme protein-modified Ni foam electrodes with that of the bare Ni foam, we performed amperometric measurements to detect H_2O_2 concentration. Fig. 7A shows the typical amperometric responses of the bare Ni foam and heme protein-modified electrodes from the addition of 50 μM H_2O_2 in 0.1 M NaOH solution under constant stirring at a fixed potential of 0.45 V (vs. Ag|AgCl).

The Ni-foam electrodes modified with heme proteins exhibited a higher current value than the bare

Ni-foam electrode. The enhanced current value of the Ni-foam electrodes modified with heme proteins could be attributed to the following:

- the exposition of more surface active sites on the surface of the 3D-porous Ni-foam electrode;
- increased wettability and surface energy of the 3D porous Ni foam;
- heme proteins did not impede the diffusion of hydroxide ions into the 3D porous network.

Among all Ni-foam electrodes modified with heme proteins, Cyt.c exhibited high and stable steady-state current response that could be due to its intrinsic electron transport bio-functionality [50].

A linear plot of the current density against the concentration of H_2O_2 was depicted in Fig. 7B. The Ni-foam electrode demonstrated a linear region from 50 μM to 450 μM with a sensitivity of 0.01 μA mM^{-1} cm^{-2}. The Hb- and Mb-modified Ni-foam electrodes showed a linear range within 50 μM to 850 μM and 50 μM to 850 μM, respectively. Their sensitivities were 0.13 and 0.16 μA mM^{-1} cm^{-2}, respectively. However, the Cyt.c-modified Ni-foam electrode showed a linear behavior from 50 μM to 950 μM, and the corresponding sensitivity was 0.39 μA mM^{-1} cm^{-2}. The synergistically enhanced electrochemical property of the Ni-foam electrodes modified with heme proteins was further determined at low H_2O_2 concentration to investigate the actual applicability. The amperometric response (Fig. 7C) of the electrodes to successive addition of 0.5 μM H_2O_2 was tested at a potential of 0.45 V (vs. Ag/AgCl). The calibration graphs for the heme-protein modified electrodes are shown in Fig. 7D. Moreover, the Cyt.c-modified Ni-foam electrode exhibited an improved level of performance in terms of detection limit, stability, and sensitivity compared with the bare Ni foam and the Hb- and Mb-modified Ni-foam electrodes (Table 2). These results demonstrated that the Cyt.c-modified Ni-foam electrode showed higher applicability than the Hb- and Mb-modified Ni-foam electrodes.

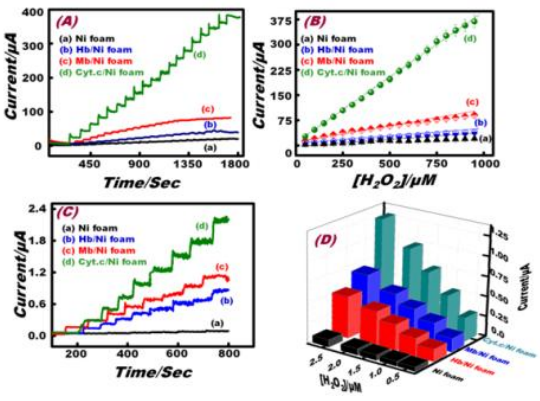

Fig. 7. – (A) Amperometric responses of the (a) bare Ni foam, (b) Hb/Ni foam, (c) Mb/Ni foam, and (d) Cyt.c/Ni foam to successive addition of 5×10^{-5} M H_2O_2 to 0.1 M NaOH solution at 0.45 V (vs. Ag|AgCl). (B) Standard calibration graph derived from the current–time plot. (C) Amperometric response of the (a) bare Ni foam, (b) Hb/Ni foam, (c) Mb/Ni foam, and (d) Cyt.c/Ni foam to successive addition of low concentration (5×10^{-7} M) H_2O_2 to 0.1 M NaOH solution at 0.45 V (vs. Ag|AgCl). (D) Standard calibration graph derived from the amperometric current–time plot at low H_2O_2 concentration.

Table 2 - Comparison of bare Ni foam and heme-protein (Hb, Mb and Cyt.c) modified Ni foam electrodes performance in terms of limit of detection, stability and sensitivity.

Sensor	Contact angle (deg)	Surface energy (mJm^{-2})	Surface tension (N/m)
Ni foam	120.45	4.40	14.40
Hb/Ni foam	109.45	8.06	19.71
Mb/Ni foam	100.05	12.35	24.87
Cyt.c/Ni foam	87.80	19.50	32.75

3.3.2 Selectivity of the Ni-foam electrodes modified with heme proteins

A sensor should have excellent selectivity because some compounds, such as DA, UA, Cyct, and AA, can interfere with signals and influence the test results. Heme proteins have become the focus of research in sensor and biosensor fields because of their satisfactory inhibitory function in addressing major interfering compounds, including DA, UA, Cyct, and AA [51]. Among the electrodes modified with heme proteins, the Cyt.c/Ni foam electrode was selected as the functional electrode to determine selectivity. Fig. 8A reveals the amperometric response of the Cyt.c/Ni foam sensor at an applied potential of 0.45 V in 0.1 M NaOH. About 5×10^{-4} M DA, 5×10^{-4} M UA, 5×10^{-4} M Cyst, 5×10^{-4} M AA, and 0.3×10^{-4} M H_2O_2 were added following the consecutive addition of 0.25×10^{-4} M H_2O_2. All potential interferences (DA, UA, Cyst, and AA) resulted in a nearly negligible amperometric response. Fig. 8 (B) shows that addition of H_2O_2 was linearly related to the presence of the interfering substances. These results showed the high selectivity of the Cyt.c/Ni foam sensor to H_2O_2. The higher selectivity of the Cyt.c/Ni foam sensor to H_2O_2 may be due to the following reasons:

The enhanced surface energy and surface tension of the Ni foam modified with heme proteins increased hydrophilicity, and the number of exposed active sites on the surface of the electrode also resulted in high sensitivity toward H_2O_2.

The strong binding efficiency (~*E*ads = 211.45 kcal mol^{-1}) of the porous Ni foam with heme proteins [52] enhanced the redox process of the modified Ni-foam sensor.

The higher diffusion of hydroxide ions and faster kinetic sensing toward H_2O_2 compared with the interferences resulted in high selectivity. This conclusion is in accordance with our previous results [53].

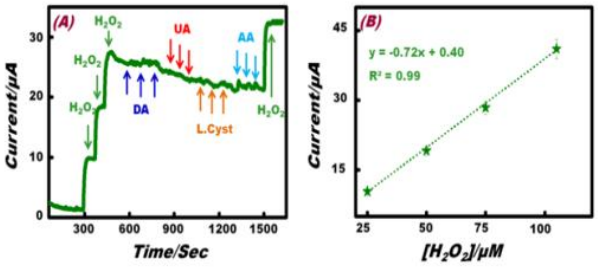

Fig. 8 – (A) Amperometric selective signal of the heme-protein (Cyt.c)/Ni foam electrode with successive addition of 0.25×10^{-4} M H_2O_2, 5×10^{-4} M DA, 5×10^{-4} M UA, 5×10^{-4} M L.Cyst., 5×10^{-4} M AA and 0.25×10^{-4} M H_2O_2 at 0.45 V (*vs.* Ag|AgCl) in 0.1 M NaOH solution. (B) The standard calibration graph derived from the current–time plot of H_2O_2 addition.

3.3.3 Real applicability of the Ni-foam electrode modified with heme proteins

Apple juice was selected as a complex matrix to confirm the performance of the developed sensor in practical applications because H_2O_2 is an important byproduct of plant and fruit juices [54]. The utilization of the proposed sensor for H_2O_2 measurement was analyzed using commercially available apple juice with a known concentration of H_2O_2. The apple juice sample was centrifuged at 40,000 rpm for 30 min, and the supernatant was used for amperometric analysis. Constant concentrations of H_2O_2 were introduced into apple juice, and the mixed samples were analyzed using standard titration and amperometric methods. The fruit sample was diluted to 1:1 with 0.1 M NaOH before analysis. Fig. 9 illustrates the typical amperometric current density response through the addition of 0.5×10^{-4} M H_2O_2 at an applied potential of 0.45 V in 0.1 M NaOH electrolyte. The small difference in the current response between the experimental and real samples was attributed to the dilution with a factor of 50%.

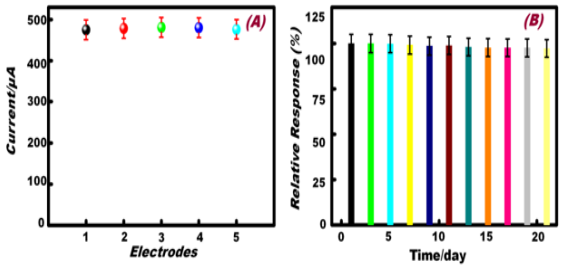

Fig. 9 – Standard calibration graph derived from the amperometric current–time plot of the Hb-, Mb-, and Cyt.c-modified electrodes to successive addition of 0.5×10^{-4} M H_2O_2 to commercially available apple juice and 0.1 M NaOH solution with 1:1 ratio at 0.45 V (vs. Ag|AgCl).

4. CONCLUSION

A worldwide demand is growing for a method that can accurately, rapidly, and selectively reorganize biomolecules, such as glucose and H2O2. In this study, non-enzymatic sensors were developed for a wide concentration range of H2O2 by immobilizing heme proteins while maintaining their biological activity onto the porous 3D Ni foam. The electrocatalytic effect of the Ni-foam electrode on H2O2 was achieved before and after modification with 100 μM heme proteins. Heme proteins mediated the electron transfer of the Ni-foam electrode by providing a high number of surface active sites, increasing hydrophilicity, and diffusing hydroxide ions for the electrooxidation of H_2O_2. The developed sensors showed remarkable sensitivity, selectivity, and linear range toward the quantification of H_2O_2. The facile, low cost, and time-saving method proposed in this study can contribute to the design and development of highly sensitive and selective electrochemical biosensors for long-term H_2O_2 in vivo measurements.

REFERENCES

1. S.A. El-Safty, M. A. Shenashen, M. Khairy, *Colloids Surf. B.* **103**, 288 (2013)
2. J. Wang, G. Chen, H. Jiang, Z. Li, X. Wang, *Analyst.* **138**, 4427 (2013).
3. S.A. El-Safty, M.A. Shenashen, M. Ismael, M. Khairy, *Chem. Commun.* **48**, 6708 (2012).
4. M. A. Shenashen, S.A El-Safty, E. A. Elshehy, *Analyst.***139**, 6393(2014).
5. S.A. El-Safty, M.A. Shenashen, M. Ismael, M. Khairy, *Adv. Funct. Mater.* **22**, 3013 (2012).
6. D. R. Rolison, J. W. Long, J. C. Lytle, A. E. Fischer, C. P. Rhodes, T. M. McEvoy, M. E. Bourg, A. M. Lubers, *Chem. Soc. Rev.* **38**, 226 (2009).
7. E.A. Elshehy, S.A El-Safty, M.A. Shenashen, *Chemosensors.* **2**, 219 (2014).
8. M.C. Henstridge, E.J.F. Dickinson, M. Aslanoglu, C. Batchelor-McAuley, R.G. Compton, *Sens. Act. B-Chem.* **145**, 417 (2010).
9. W.A. El-Said, J. Lee, B. Oh, J. Choi, *Electrochem. Commun.* **12**, 1756 (2010).
10. M. Khairy, S. A El-Safty, M. Ismael, *Chem. Commun.* **48**, 10832 (2012).
11. C. Yuan, L. Yang, L. Hou, L. Shen, X. Zhang, X. W. Lou, *Energy Environ. Sci.* **5**, 7882 (2012).
12. M. Grden, M. Alsabet, G. Jerkiewicz, *ACS Appl. Mater. Interfaces.* **4**, 3012 (2012).
13. J. Xiao, S. Yang, *RSC Adv.* **1**, 588 (2011).
14. M. Khairy, S. A El-Safty, *Chem. Commun.* **50**, 1356 (2014).
15. G.R. Moore, R.J.P. Williams, *Eur. J. Biochem.* **103**, 513 (1980).
16. K. Kao, C. Lee, T. Lin, C. Mou, *J. Mater. Chem.* **20**, 4653 (2010).
17. S.S.K. Wijeratne, S.L. Cuppett, V. Schlegel, *J. Agric. Food Chem.* **53**, 8768 (2005).
18. L. Wang, E. Wang, *Electrochem. Commun.* **6**, 225 (2004).
19. J.E. Erman, L.B. Vitello, J.M. Mauro, J. Kraut, *Biochemistry.* **28**, 7992 (1989.)
20. M. Zhou, Z. Diwu, N. Panchuk-Voloshina, R.P. Haugland, *Anal. Biochem.* **253**, 162 (1997).
21. A.N. Diaz, M.C.R. Peinado, M.C.T. Minguez, *Anal. Chim. Acta.* **363**, 221 (1998).
22. S. Yabuki, F. Mizutani, Y. Hirata, *Sens. Act. B-Chem.* **65**, 49 (2000).
23. H.A. Khorami, J.F. B. Cadavid, P. Wild, N. Djilali, *Electrochim. Acta.* **115**, 416 (2014).
24. Y. Guo, J. Li, S. Dong, *Sens. Act. B-Chem.* **160**, 295 (2011).
25. B. Haghighi, R. Nikzad, *Electroanalysis.* **21**, 1862 (2009).
26. R. Cui, Z. Han, J. Zhu, *Chem.--Eur. J.* **17**, 9377 (2011).
27. A.A. Ensafi, M. Jafari-Asl, N. Dorostkar, M. Ghiaci, M. Martinez-Huerta, J.L.G. Fierro, *J. Mater. Chem. B.* **2**, 706 (2014).
28. B. Luo, X. Li, J. Yang, X. Li, L. Xue, X. Li, J. Gu, M. Wang, L. Jiang, *Anal. Methods.* **6**, 1114(2014).
29. S.A.G. Evans, J.M. Elliott, L.M. Andrews, P.N. Bartlett, P.J. Doyle, G. Denuault, *Anal. Chem.* **74**, 1322 (2002).
30. N. Akhtar, S. A El-Safty, M. Khairy, W.A. El-Said, *Sens. Act. B-Chem.* **207**, 158 (2015).
31. N. Akhtar, S.A El-Safty, M. Khairy, *Chemosensor.* **2**, 235 (2014).
32. J. P. Rinuy, P. Brevet, H.H. Girault, *Phys. Chem. Chem. Phys.* **4**, 4774 (2002).
33. C.W. Ong, Z.X. Shen, K.K.H. Ang, U.A.K. Kara, S.H. Tang, *Appl. Spectrosc.* **53**, 1097 (1999).
34. B.R. Wood, S.J. Langford, B.M. Cooke, F.K. Glenister, J. Lim, D. McNaughton, *FEBS Lett.* **554**, 247 (2003).
35. K. Ramser, K. Logg, M. Goksor, J. Enger, M. Kall,

D. Hanstorp, *J. Biomed. Opt*. **9**, 593 (2004).
36. B.R. Wood, D. McNaughton, *Biopolymers* **67**, 259 (2002).
37. S. Hu, K.M. Smith, T.G. Spiro, *J. Am. Chem. Soc.* **118**, 12638 (1996).
38. K. Hamada, K. Fujita, N.I. Smith, M. Kobayashi, Y. Inouye, S. Kawata, *J. Biomed. Opt*. **13**, 044027 (2008).
39. S. Hu, I.K. Morris, J.P. Singh, K.M. Smith, T.G. Spiro, *J. Am. Chem. Soc.* **115**, 12446 (1993).
40. S. Wu, W. Tan, H. Xu, *Analyst*. **135**, 2523 (2010).
41. X. Lu, X. Xiao, Z. Li, F. Xu, H. Tan, L. Sun, L. Wang, *Anal. Methods* **6**, 235 (2014).
42. Q. Yan, Z. Wang, J. Zhang, H. Peng, X. Chen, H. Hou, C. Liu, *Electrochim. Acta*. **61**, 148 (2012).
43. M. Fleischmann, K. Korinek, D. Pletcher, *J. Electroanal. Chem. Interfacial Electrochem*. **31**, 39 (1971).
44. F. Yang, K. Cheng, X. Xue, J. Yin, G. Wang, D. Cao, *Electrochim. Acta*. **107**, 194 (2013).
45. K. Murata, M. Suzuki. N. Nakamura, H. Ohno, *Electrochem. Commun.* **11**, 1623 (2009).
46. R.E. Johnson, R. H. Dettre, *Wetteability* (New York: Dekker: 1993).
47. D.Y. Kim, J.Y. Kim, H. Chang, M.S. Kim, J. Leem, J. Ballato, S. Kim, *Nanotechnology* **23**, 485606 (2012).
48. A.J. Bard, L.R. Faulkner, Electrochemical methods: Fundamentals and applications, second ed. (Wiley: New York: 2001).
49. A. Bunea, I. Pavel, S. David, S. Gaspar, *Chem. Commun.* **49**, 8803 (2013).
50. Q. Li, G. Luo, J. Feng, *Electroanalysis*. **13**, 359 (2001).
51. X. Liu, J.L. Zweier, *Free Radic. Biol. Med*. **31**, 894 (2001).
52. M. Khairy, S. El-Safty, *Chem. Commun*. **48**, 10832 (2012).
53. S.A. El-Safty, A.A. Ismail, H. Matsunaga, T. Hanaoka, F. Mizukami, *Adv. Funct. Mater*. **18**, 1485 (2008).
54. S. Lu, J. Song, L. Campbell-Palmer, *Sci. Hortic-Amsterdam*. **120**, 336 (2009).